NASA Contractor Report 3618

Theoretical Studies of Radiation Effects in Composite Materials for Space Use

C. Ken Chang and Efstathios Kamaratos

GRANT NSG-1614
SEPTEMBER 1982

NASA Contractor Report 3618

Theoretical Studies of Radiation Effects in Composite Materials for Space Use

C. Ken Chang and Efstathios Kamaratos
Christopher Newport College
Newport News, Virginia

Prepared for
Langley Research Center
under Grant NSG-1614

National Aeronautics
and Space Administration

**Scientific and Technical
Information Branch**

1982

Page intentionally left blank

Page intentionally left blank

TABLE OF CONTENTS

LIST OF TABLES

LIST OF FIGURES

INTRODUCTION

It is known that polymeric matrix materials meet the structural requirements for large space structures (Ref. 1), but the strength of these materials is adversely affected by long term radiation exposure in space environment (Ref. 2) and questions still remain regarding their long-term stability (Ref. 3). In order to facilitate large structure feasibility and design studies, especially for a 30-year geostationary mission, data on degradation of matrix materials subject to space environment must be obtained.

Our research efforts have been directed towards several important areas: 1) computer programming on energy deposition calculations for a model polymer in space environment, 2) a feasibility study of space flight accelerated testing, and 3) theoretical study of interaction between charged particles and some compounds of interest. In the following paragraphs brief descriptions of these areas are given and the results are presented and discussed.

1. Computer Programming

Graphite epoxy composites have been suggested (Ref. 6) for space application due to their desirable physical characteristics such as high stiffness and small thermal distortion. In the present study, tetraglycidyl 4,4'-diamino diphenyl methane epoxy cured with diamino diphenyl sulfone (Fig. 1) is chosen as a model compound (Ref. 3). Fortran IV Programs have been developed to calculate some quantities of importance to the study of this polymer when subject to electron and proton irradiation, an environment exist in space.

The stopping power and range of the composite depend on the energy of incident particles. The program is capable of computing these values as a function of incident

particle energy and composition of the composite. Table I shows the calculated results for a typical graphite epoxy composite (30% epoxy by volume) as an example. Energy deposition coefficients for electrons and protons in target materials are of course depending on incident particle energy. This dependency is shown in Figures 2 and 3. Fig. 4 compares the penetration depth of electrons and protons at various incident energies as derived from Ref. 4 and 5. The unit of depth in g/cm^2 can be converted to cm by taking the density range of the composite to be $1.5 \sim 1.7$ g/cm^3 (Table 2). This range is calculated from the density of the epoxy being 1.3 g/cm^3 (Ref. 3) and $1.6 \sim 1.9$ g/cm^3 for graphite fibers prepared by graphatizing either rayon or polyacrylonitril fibers (Ref. 7).

Figure 5 shows an accumulated dose in the composite exposed to charged particle environment in geosynchronous orbit for 30-year duration. The upper and lower limits in this plotting show uncertainties of the environment involved. The shaded band shows the difference in dose received by composite due to difference in geometry of the object, i.e., a spherically shaped object receives a larger dose while the dose is less for a semi-infinite material slab in the same environment. The program uses fluence spectrum at the given altitude and inclination as input and computes dose received at various depths. Figures 6 and 7 show, respectively, examples of electron and proton doses received in the composite when it is placed in an orbit of 1,000 Km altitude and 30° inclination. Environmental models AE4 and AE5 were used for fluence spectrum.

Some of these values and graphs will be used in subsequent discussions.

2. Accelerated Testing

Despite the enthusiasm for epoxy as the binder of graphite fibers in large space structure applications, questions still remain regarding its long-term stability as noted earlier. It is clear that more detail studying of degradation and testing under a simulated condition must be conducted and results analyzed. Perhaps the most feasible study for this purpose is through accelerated testing (Ref. 8,9).

Accelerated testing will likely take two forms: (1) ground based laboratory testing, and (2) low earth orbit flight testing with an LDEF type vehicle. Although ground testing is limited in its ability to simulate launch and space environment, it has many advantages. Tests may be conducted rapidly and inexpensively with radiation producing machine on the materials presently on market or on new ones as they become available. Sophisticated instruments are available for analyzing, as the sample is being irradiated, evolving gases, detecting and possibly identifying reactive species such as excited molecules, ions and radicals produced in the bulk of the material. This information is vital in developing a model in understanding the initial phase of physical interaction between ionizing particles and composite materials, and in explaining the subsequent chemical evolution. The value of this analytical model lies in its potential use not only for basic understanding of radiation effects on polymeric materials, but also for evaluating adequacy of accelerated testing, and for providing a better basis in predicting useful life of a large space structure. On the other hand, in low earth orbit flight testing, little or no such diagnostic test may be performed during exposure, but the space and launch environment can be produced with fair accuracy for geosynchronous mission. Retrieved samples from such a testing can be analyzed in the laboratory and will certainly provide invaluable information on degradation of materials in a near perfect environment.

A preliminary analysis has been conducted to determine a low earth orbit which has such a radiation environment that in a rather short period of time, a sample placed in this orbit could accumulate enough radiation dose equivalent to a 30-year geosynchronous orbit. Further, such an orbit should be accessible to Shuttle/orbiter for retrieving irradiated sample for detail analysis in a laboratory. The present analysis has been limited to data from AE2, AP5 and AP6 environmental models in lieu of more recent data (Ref. 10) which has not been available.

2-1. Calculation Methods

The model compound used in this study is as shown in Fig. 1. This compound is used to bind graphite fibers in forming the composite. A typical composition of this type of composite is 70% graphite and 30% epoxy by volume. The density range has been calculated for the composite and is shown in Table 2.

The energy absorbed by the composite at a depth x due to incident particles with fluence $\phi(E)$ is

$$D(x) = \int_0^\infty \xi(E,X)\ \phi(E)dE \qquad (2\text{-}1)$$

where $\xi(E,X)$, the energy deposition coefficient, for normal incident particles on a sheet of the material is shown in Figures 2 and 3. The significance of these figures will be discussed later. The main objective of this study is to seek a low-earth orbit whose dose would match that of geosynchronous orbit shown in Fig. 5 in a reasonably short period of time.

The dose rate as a function of altitude for circular orbits as calculated in Ref. 10 is used. Figures 8 and 9 show, respectively, electron and proton dose rate in composite material exposed in circular orbits at zero-inclination. The long-term average dose rate for arbitrary orbits can be found by using the averaged exposure for circular orbit data of the time varying altitude and averaging over one revolution (Ref. 11). The orbit

equations are solved by evaluating the orbital angular momentum and integrating the corresponding force equations. The average dose is

$$D(r_a, r_p) = \frac{1}{\tau} \int_0^{\tau} D[r(t)]dt \qquad (2\text{-}2)$$

where r_a and r_p are the orbit apogee and perigee, τ is the orbital period, and t is time.

2-2. Results

Calculations of dose received by the composite have been made by taking the apogee at the peak of the inner electron radiation zone approximately at 270 Km altitude, and increasing perigee from Shuttle - accessible altitudes until the perigee reaches the peak of the inner electron belt when the orbit becomes circular. The results for 2-year exposure are shown in Fig. 10. From this figure, it is clear that the radiation dose received by the composite at the depth of 3 to 6 mils in the geosynchronous environment for 30 years can be accumulated in two years or less when it is placed in an elliptical equitorial orbit of 300 Km perigee by 2750 Km apogee.

In regard to proton radiation, the high surface doses cannot be achieved at the peak altitudes of the inner electron belt. It would be necessary to increase the apogee to 10,000 Km to sample the low energy proton as indicated by zero depth curve in Fig. 10.

Other factors affecting the dose rate such as the height of perigee and orbital inclination are discussed in a publication (Ref. 12).

3. Theoretical Studying of the Model Compound

A compound, tetraglycidyl 4,4'-diamino diphenyl methane epoxy cured with diamino diphenyl sulfone as shown in Fig. 1, is used as a model compound to further study on radiation damage to polymeric composite materials. Unlike crystalline materials where nuclear displacement plays an important role, damages received by polymers due to charged particles are largely due to chemical evolution of excited species produced in the initial phase of interaction. In complex molecules, such as the polymeric system we are considering, energy thus received is usually shared by many vibrational modes through intricate potential surface crossings which is intimately related to molecular structure. A better understanding of energy deposition mechanism and the formation of excited species, some of which are long lived due to lack of mobility in solid state, are of utmost importance in understanding the final chemical products observable in a laboratory.

3-1. Energy Deposition

Energy transferred by an energetic charge particle to a target is given by Bethe equation:

$$\frac{dE}{dx} = \frac{4\pi N z^2 e^4}{M v^2} \sum_n f_n \ell n \frac{2Mv^2}{E_n} \tag{3.1}$$

where N and e are number of particles in a unit volume and electric charge, respectively, M and v are the mass and velocity of the charge particle, while z is the atomic number of the target. The passing coulomb field from the particle appears as a field of virtual photons is evidenced by the strong dependency of the stopping power, dE/dx, on the optical dipole oscillator strengths f_n and the corresponding excitation energy levels E_n of the target. Molecular geometry and chemical bonding are intricately related to these quantities and they are related to the mean excitation energy I:

$$Z \ell n I = \sum_{n=1}^{\infty} f_n \ell n(E_n) \tag{3.2}$$

Detailed calculation of excitation energies and oscillator strengths of polymers is not feasible at present and a suitable approximation method will be very desirable. Local plasma approximation (Ref. 12) is such a method whereby the molecule is replaced by a space dependent plasma. With this approximation, the mean excitation energy I and total number of electrons Z are related to the electron density $\rho(\vec{r})$ of the molecule and the local plasma frequency $\omega(\vec{r})$ as

$$Z \ln (I) = \int \rho(\vec{r}) \ln[\gamma h\omega(\vec{r})] \, d^3 \vec{r} \tag{3.3}$$

where the local plasma frequency $\omega(\vec{r})$ is

$$\omega(\vec{r}) = [4\pi e^2 \rho(\vec{r})/m]^{1/2} \tag{3.4}$$

where e is the electron charge, m is the electron mass, and the parameter γ taken approximately as 1.2 (Ref. 13). Within the context of the Gordon-Kim electron gas approximation, the mean excitation energies of several covalent molecules have been calculated by applying the local plasma approximation (Ref. 14). These values compare very favorably with the experimental-empirical values as can be seen in Table 3. Bragg's rule values are obtained from applying the Bragg's rule to accurate atomic values calculated by Dehmer, et al. The discrepancies between Bragg's and experimental values are clearly due to chemical bond effects.

Ionic bonding effects on the mean excitation energy were also studied via local plamas model on LiF, LiH and HF molecules (Ref. 15). Again, following Gordon-Kim model for electron density for these diatomic molecules the electron density at $\vec{r}$ is calculated:

$$\rho_p(\vec{r}) = \rho_A(+p) \, (\vec{r}) + \rho_B(-p) \, (\vec{r}-\vec{R}) \tag{3.5}$$

where $A^{(+p)}$ and $B^{(-p)}$ refer to the partially ionic states of A and B, the two constituent atoms, R is the internuclear distance and p is the ionic fraction. The electron density of a partial ionic atom A in equation (3.5) is

$$\rho_A(\pm p) = (1-P) \, \rho_A(\vec{r}) + P \, \rho_{A^{\pm}}(\vec{r}) \tag{3.6}$$

where $\rho_A(\vec{r})$ and $\rho_{A^{\pm}}(\vec{r})$ are the electron densities of atomic neutral and atomic ionic states, respectively, of A. Appropriate atomic wave functions, nuclear distances and ionic fractions are used to calculate the mean excitation energy I in Table 4. From this table, it is seen that the main contribution to correction to the Bragg rule is the adjustment from atomic neutral mean excitation energy to atomic ion mean excitation energy.

3-2. Study of Bond Rupture Sites

The energy imparted by a passing charged particle excites a molecule into its excited electronic, vibrational and rotational states. These lead to subsequent production of stable excited species and fragments due to bond rupture. In search of empirical information which may provide a better basis for predicting fragmentation formation of our model polymer, we examined electron-impact mass spectroscopic data on molecules which have the same functional groups as does the model (Fig. 1).

Mass spectra of many molecules containing amino functional groups are obtained (Ref. 16). It has been observed that among several functional groups, including hydroxyl and amino groups, that are present as substituents in aliphatic compounds, the amino group has the strongest influence on the site of bond scission and ionization due to electron impact (Ref. 17,18). The extent of substitution on the amino group itself appears to increase the influence of the amino group on its directive dissociative ionization. The dominant bond scission in the presence of amino group is between α and β carbon atoms in hydrocarbon chains, leading to the formation of immonium ions.

The presence of a hydroxyl group in an aliphatic compound appears to favor scission of bond between α and β carbon atoms, although the influence is not so strong as that of the amino group. When both the amino and the hydroxyl group are present in a molecule, the amino group appears to form a more abundant fragment ion (immonium ion)

compared to oxonium ion from hydroxyl group. When a sulfonyl group is present in a molecule, its mass spectrum shows ions formed by scission of C-S and S-O bonds.

Based on the study of mass spectra of compounds containing functional groups as appear in our model compound, we predicted the sites of possible major ionization and bond scission in the model compound when subject to irradiation by high energy electrons (Fig. 11). The transient species observed in pulse radiolysis experiments conducted by JPL bore out these predictions.

3-3. Density Distribution of Excited Species

The energy lost when a moving charged particle is slowed down in matter gives rise to a trail of excited and ionized atoms and/or molecules in the path of the particle. Radiation of different types and energy will lose energy in matter at different rates, and consequently will form tracks in condensed media that may be densely or sparsely populated with active species. This difference in density of active species produced in the media, leads to differences observed in the chemical effect of different radiation.

A comparison has been made for logitudinal energy absorption for monoenergetic protons and electrons penetrate into the epoxy and graphite epoxy composite (Figures 2 and 3). The energy deposition per unit volume is high for protons and results in shorter penetration depth. On the other hand, electrons penetrate deeper into media with declining peak values due to increased multiple scattering at larger depths.

The lateral dispersion of the energy deposit extends over two energy absorption regions, the core and the penumbra. In the core, the energy transferred from a passing charged particle to a material shows radial dependence that depends on the mechanism of the coulombic interaction considered. One process involves the coulombic interaction

between the charged particle and the electron of one individual atom or molecule, in which case the radial dependence of the energy transferred is given approximately (Ref. 19a) by equation (3.7). Another process involves the collective longitudinal excitation of valence electrons of the atoms or molecules in the condensed phase, in which case the radial dependence is given approximately (Ref. 19b) by equation (3.8) (for singly charged projectiles)

$$P_n \approx \exp(-E_n r/3hv), \tag{3.7}$$

$$\rho(r) \approx \exp(-2\omega_p r/v)/r^2. \tag{3.8}$$

Clearly, the highest energy transfers are restricted to small radial distances. Even so the highest energy transfers result in energetic secondary electrons which generally travel far from their sites of production and depositing their energy far from the trajectory of the original passing particle forming a penumbra of energy deposit outside the core region. The core and penumbra of 100 KeV protons and electrons are shown clearly in the graph (Fig. 12). The core region of the proton is limited to a few atomic distances by the proton's low velocity, while the electron core to about 6 nm according to equation (3.7). The proton-produced penumbra is limited by the secondary electron mass to proton mass ratio, which limits the energy transferred to secondary electrons. The electron produced penumbra extends far off the graph to the right. There are great differences between the excitation densities achieved by the passage of the two particles. Without doubt, rapid recombination will characterize the chemistry in the proton's core region. A more detailed analysis is required to better define the chemistry of these various regions of exposure.

At higher particle energy the same features are apparent in the track structure but the radial distances are expanded (Fig. 13). The proton core region still appears on the graph but the electron core extends to the right of the present graph. Qualitatively, we anticipate the proton core chemistry to be radically different from the remainder of the exposed regions. The chemical change in any solid material will be

limited to a small cylindrical region around the individual particle trajectory. Early in the exposure these cylindrical regions will not overlap and their evolution develop independently of one another. Late in the exposure of highly irradiated material the chemistry of later tracks will generally be altered by the prior change of the material caused by a previous track.

Another important factor one should consider is the frequency of the passage of charged particles through a given region. The accumulated 30-year dose for geostationary orbit is shown in Figure 5. It is represented by exposure of $\approx 10^{11}$ rad at ≈ 0.5 μ depths due to low energy protons and $\approx 5 \times 10^{9}$ rad at ≈ 50 μ due to electrons. At these values, each portion of material receives energy by the near passage of several particles. Two effects could result from such multiple track exposure: (a) if sufficiently close in time, then chemically active species of the two trajectories may alter the chemical end product; (b) even if long times elapsed between the passage of the two particles then the second passes through previously altered material. Of interest is the number of traversals which overlap within a given time interval for an accelerated test of the 30-year geostationary exposure.

The probability of overlap of two particle tracks within a time interval Δt is shown for an accelerated test at 30-year geostationary exposure levels (Table 5). The test is assumed completed in one day (24 hours). It is seen that the more active chemical species ($\Delta t \approx 1$ μsec) will rarely be affected by such events. A small effect is expected for the slow chemical processes ($\Delta t \approx 1$msec) in the penumbra region of the electron exposure. Effects on long lived radicals ($\Delta t = 1$ sec) is likely in nearly all regions. Most of the exposure is seen to take place in previously disturbed material ($\Delta t \approx 1$ day). What is clear from these figures is that material changes result from the combined effects of spatially compact individual particle tracks.

4. Conclusion

Our efforts have been directed toward the study of graphite epoxy composite and its utilization in building a large space structure for future geosynchronous missions. We have assisted in completing versatile computer programs which enabled us in obtaining important information with regard to interaction between graphite epoxy composite and charged particles which are present in the space environment. We have considered accelerated testing of the composite by placing samples in low earth orbits accessible to Shuttle/orbitor for subsequent retrieval. It is found that an elliptical equitorial orbit of 300 Km perigee by 2750 Km apogee can accumulate, in two years or less, enough radiation dose comparable to geosynchronous environment for 30 years.

In theoretical studies of radiation damage to epoxy materials, we have applied local plasma model to calculate the mean excitation energy for both covalent and ionic compounds. The mean excitation energy is an important quantity in calculating the stopping power (and hence range) of charged particles in a medium and has been obtained from experimental results. It is extremely encouraging to see good agreement between local plasma model and experimental results. We also conducted an extensive literature search on electron-impact mass spectroscopy of compounds which have functional groups similar to those present in the model polymer. From this vast amount of information we were able to identify possible sites of bond rupture in the model polymer and succeeded in predicting formation of radicals observed in preliminary experiments conducted at JPL and reported recently. Density distribution of excited species produced by charged particles penetrating the media is studied. We considered both longitudinal and lateral distributions of excited species by both electrons and protons. The probability of overlapping of two tracks due to two charged particles within various time intervals is calculated. Unlike gaseous media, reactive species produced in condensed media, in general, are lacking in mobility, hence track effects are more important in condensed media.

5. Future Work

We are planning to investigate the formation of anions due to electron impact and study the effects of these ions in materials when placed in space environment. Formation of ions due to proton impact and their role in degradation of materials need to be investigated also. Further, the study of situation in which the polymer is subject to simultaneous irradiation by both electrons and protons is needed.

Thermal effects on material subject to ionization radiation are not clear. Due to lacking of mobility of polymer molecules, high LET will undoubtedly create high temperature zones in the tracks. Possibilities of thermal decomposition of radicals as an added mechanism for decomposition of irradiated acetone has been suggested (Ref. 20). Thermal effects may prove to be an important factor especially in accelerated testing of the polymer.

With the success in applying local plasma model to some molecules, we intend to apply this model to molecules of interest and to our model polymer with appropriate approximation. The mechanism of transferring energy of excitation throughout the polymer molecule is not clear. Molecular exciton theory has been applied and has met some successes. The mechanisms of interaction between a molecule and a charged particle, and subsequent energy transfer will elucidate the paths by which excited species are formed.

A modeling of reaction will be attempted for excited species produced by charged particle irradiation. It will be interesting to estimate the half-life and reaction rates of these species in order to enhance our understanding of pathways by which our model polymer degrades.

Acknowledgments

Numerous assistances generously provided by Dr. John W. Wilson of NASA/LaRC are gratefully acknowledged. The assistances in some computations provided by Mr. Y. J. Xu and Mr. L. V. Stock, both of Old Dominion University, are very much appreciated.We also express our appreciation to the members of Space Technology Branch, NASA/LaRC, who provided us with an excellent environment in conducting this investigation.

References

1. Powell, Denis J., and Browning, Lee: "Automated Fabrication of Large Space Structures." Astronautics and Aeronautics, vol. 16, p. 30, 1978.

2. Nuclear and Space Radiation Effects on Materials. NASA SP-8053, 1970.

3. Long, Edward R.: "Electron and Proton Absorption Calculations for a Graphite/Epoxy Composite Model." NASA TP-1568, November 1979.

4. Anderson, H. H., and Zeigler, J. F.: Hydrogen Stopping Powers and Ranges in All Elements. Pergamon Press, New York, 1977.

5. Berger, M. J., and Seltzer, S. M.: Tables of Energy Losses and Ranges of Electrons and Positrons. NASA SP-3012, 1964.

6. Goudwin, Charles J.: Space Platforms for Building Large Space Structures. Astronautics and Aeronautics, vol. 16, p. 44, 1978.

7. Galasso, F. S.: High Modulus Fibers and Composites. Gordon and Breach, Science Publishers, New York, 1969.

8. Card, M. F., Kruszeqski, E. T., and Guastaferro, A.: Technology Assessment and Outlook. Astronautics and Aeronautics, vol. 16, p. 48, 1978.

9. Tenney, D. R., Slemp, W. S., Long, E. R., Sykes, G. F., and Stein, B. A.: Space Environmental Effects on Composite Materials--Assessment and Research Needs. Presented at the 12th AIAA Fluid and Plasma Dynamics Conference, Williamsburg, VA, July 23-25, 1979.

10. Cladis, J. B., Davidson, G. T., and Newkirk, L. L.: The Trapped Radiation Handbook. DNA 2524H, Washington, DC, December 1971.

11. Wilson, J. W., Stock, L. V., Carter, D. J., and Chang, C. K.: Preliminary Analysis of Accelerated Space Flight Ionizing Radiation Testing. NASA TM-83209, 1982.

12. Lindhard, J., and Scharff, M.: Recent Development in the Theory of Stopping Power. 1. Principles of Statistical Method. National Academy of Science-National Research Council Publication 752, pp. 49-52, 1960.

13. Chu, W. C., and Powers, D.: Calculation of Mean Excitation Energy for All Elements. Physics Letters, vol. 40, p. A23, 1972.

14. Wilson, J. W., and Kamaratos, E.: Mean Excitation Energy for Molecules of Hydrogen and Carbon. Physics Letters, vol. A85, p. 27, 1981; and references therein.

15. Wilson, J. W., Chang, C. K., Xu, Y. J., and Kamaratos, E.: Ionic Bond Effects on the Mean Excitation Energy for Stopping Powers. Journal of Applied Physics, vol. 53, no. 2, p. 828, 1982; and references therein.

16. Heller, S. R., and Milne, G. W. A. (editors): EPA/NIH Mass Spectral Data Base--1980 Cumulative Indexes. NSRDS-NBS 63, Supplement 1.

17. Remberg, G., Remberg, E., Spiteller-Friedmann, M., and Spiteller, G.: Massenspektren Schwach Angeregter Molekule. 4 Miteilung Org. Mass. Spectrom., vol. 1, pp. 87-113, 1968.

18. Remberg, G., and Spiteller, G.: Uber den Einfluss von Substituenten Auf die Primaren Abbaureaktionen Aliphatischer Verbindungen im Massenspectrometer. Chem. Ber., vol. 103, pp. 3640-3660, 1970.

19. Wilson, John W.: Solar-Pumped Gas Laser Development. NASA TM-81894, December 1980.

20. Ritchie, R. H., and Brandt, Werner: Primary Processes and Track Effects in Irradiated Media. Radiation Research--Biomedical, Chemical, and Physical Perspectives. Academic Press, Inc., pp. 315-324, 1975.

21. Matsui, M., and Imamura, M.: Radiation Chemical Studies with Cyclotron Beams. III. Heavy Ion Radiolysis of Liquid Aliphatic Ketones. Bulletin of the Chemical Society of Japan, vol. 47, p. 1113, 1974.

TABLE I

ENERGY, RANGE AND STOPPING POWER OF GRAPHITE EPOXY (30% EPOXY)
BY PROTON AND ELECTRON IMPACTS FOR THE ENERGY RANGE OF 0.01 TO 10 MeV

	Electron		Proton	
Energy (MEV)	Range (G/CM^2)	Stopping Power ($MEV \cdot CM^2/G$)	Range (G/CM^2)	Stopping Power ($MEV \cdot CM^2/G$)
.100E-01	.307E-03	.198E+02	.230E-04	.624E+03
.200E-01	.985E-03	.118E+02	.434E-04	.556E+03
.300E-01	.199E-02	.865E+01	.601E-04	.642E+03
.400E-01	.329E-02	.696E+01	.749E-04	.698E+03
.500E-01	.485E-02	.591E+01	.889E-04	.731E+03
.600E-01	.666E-02	.519E+01	.102E-03	.748E+03
.700E-01	.870E-02	.467E+01	.116E-03	.754E+03
.800E-01	.109E-01	.427E+01	.129E-03	.752E+03
.900E-01	.134E-01	.394E+01	.142E-03	.743E+03
.100E+00	.160E-01	.368E+01	.156E-03	.731E+03
.200E+00	.509E-01	.251E+01	.310E-03	.574E+03
.300E+00	.945E-01	.212E+01	.505E-03	.468E+03
.400E+00	.144E+00	.191E+01	.737E-03	.400E+03
.500E+00	.198E+00	.179E+01	.100E-02	.353E+03
.600E+00	.255E+00	.173E+01	.130E-02	.317E+03
.700E+00	.313E+00	.170E+01	.163E-02	.289E+03
.800E+00	.372E+00	.168E+01	.200E-02	.266E+03
.900E+00	.432E+00	.165E+01	.239E-02	.247E+03
.100E+01	.493E+00	.161E+01	.281E-02	.229E+03
.200E+01	.111E+01	.162E+01	.857E-02	.141E+03
.300E+01	.171E+01	.165E+01	.169E-01	.104E+03
.400E+01	.230E+01	.167E+01	.277E-01	.838E+02
.500E+01	.287E+01	.168E+01	.408E-01	.706E+02
.600E+01	.344E+01	.169E+01	.560E-01	.612E+02
.700E+01	.401E+01	.168E+01	.734E-01	.542E+02
.800E+01	.457E+01	.167E+01	.929E-01	.488E+02
.900E+01	.514E+01	.165E+01	.114E+00	.444E+02
.100E+02	.571E+01	.162E+01	.138E+00	.408E+02

TABLE 2

DENSITY OF GRAPHITE FIBERS, EPOXY AND COMPOSITE MATERIALS
WITH 70% GRAPHITE AND 30% EPOXY (BY VOLUME)

	Graphite Fibers[7]	Epoxy[3]	Composite
density, g/cm^3	1.6~1.9	1.32	1.5~1.7

TABLE 3

MEAN EXCITATION ENERGY (eV) OF COVALENT COMPOUNDS

	Present Theory	Experimental-Empirical	Bragg's Rule
CH_4	44.7	42.8	35.1
$(CH_2)_x$	55.0	53.4	43.5
C_6H_6	60.6	61.4 ± 1.9	50.6
H_2	18.9	18.5 ± .5	15.0
graphite	76.1	78.5 ± 1.5	62.0

TABLE 4

IONIC BOND PARAMETERS
(UNITS OF MEAN EXCITATION ENERGY ARE eV)

	HF	LiH	LiF
I	96.4	26.7	93.6
I_{Bragg}	91.0	25.9	81.6
$I_{ionic\ Bragg}$	91.7	25.2	92.6
$I_{covalent}$	97.6	27.8	83.4
P	0.50	0.25	0.90
R,Å	0.91	2.04	2.04

TABLE 5

PROBABILITY OF OVERLAP OF TWO-PARTICLE TRACKS WITHIN TIME ΔT
(30-YEAR GEOSTATIONARY EXPOSURE ACCELERATED BY 10^4)

	PROTON		ELECTRON	
ΔT	CORE	PENUMBRA	CORE	PENUMBRA
1 μsec	3×10^{-11}	3×10^{-8}	5×10^{-7}	2×10^{-5}
1 msec	3×10^{-8}	3×10^{-5}	5×10^{-4}	2×10^{-2}
1 sec	3×10^{-5}	3×10^{-2}	5×10^{-1}	≈ 1
1 day	≈ 1	≈ 1	≈ 1	≈ 1

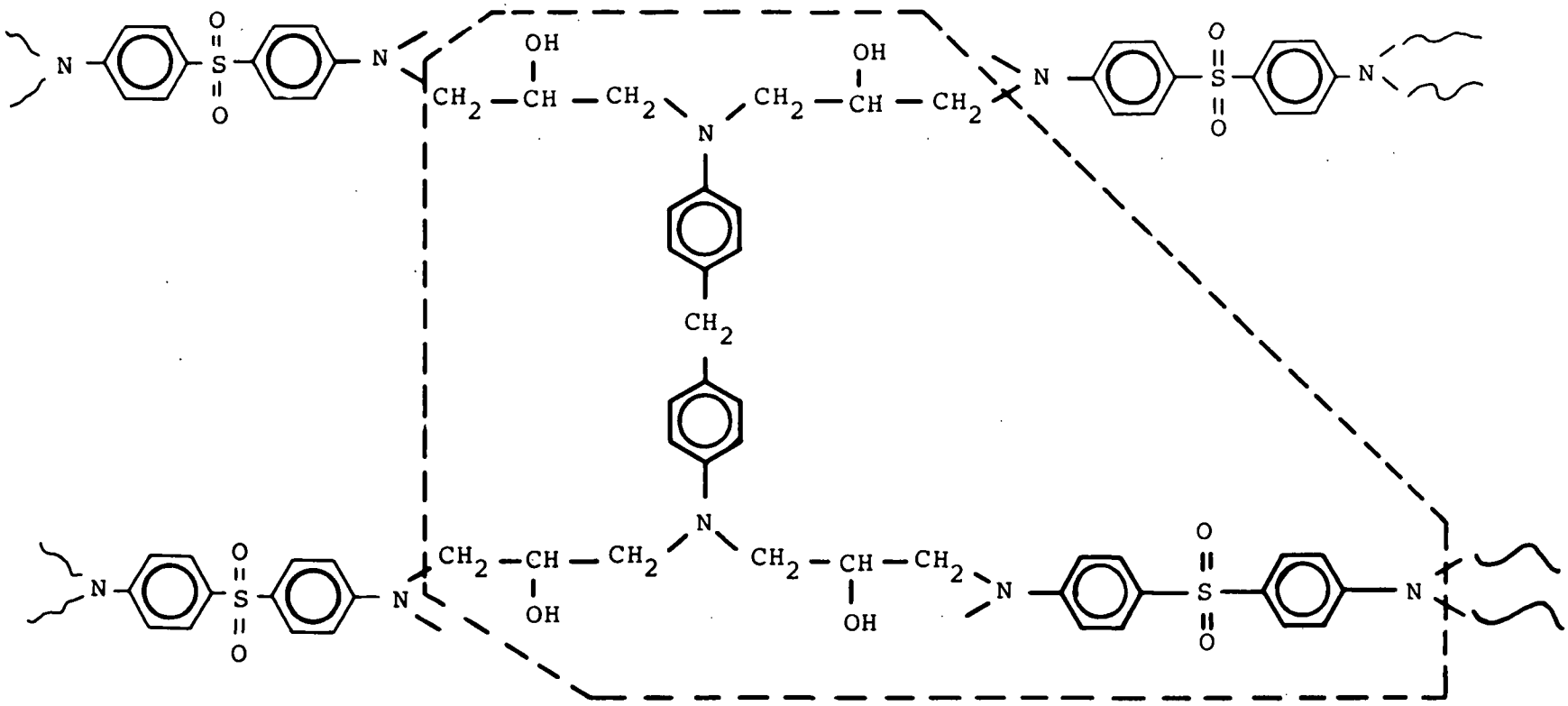

Fig. 1. Tetraglycidyl 4, 4' - diamino diphenyl methane epoxy cured with diamino sulfone. The dashed line encloses the repeat cured unit.

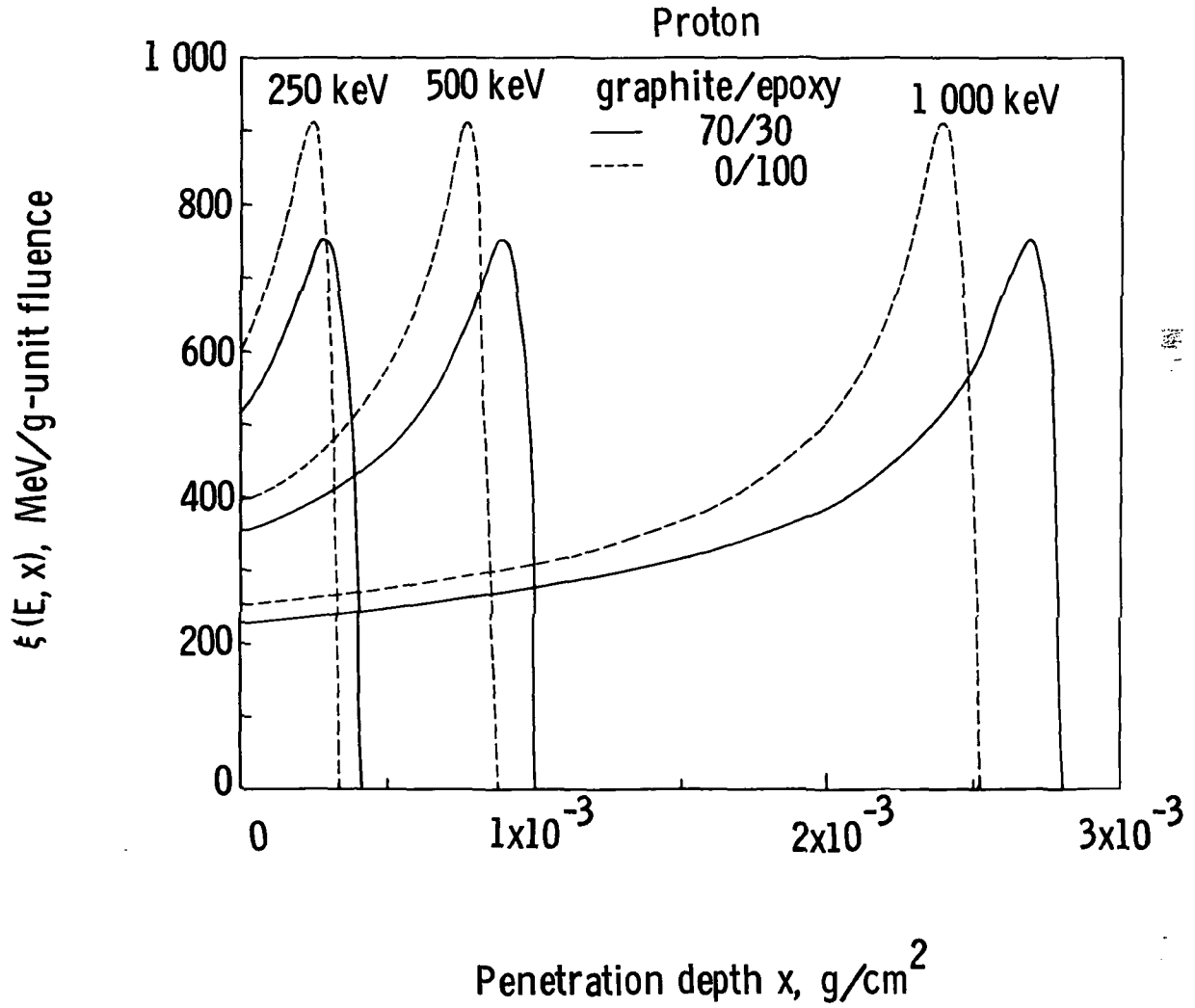

Fig. 2 - Proton energy deposition coefficient for graphite epoxy composite and pure epoxy material.

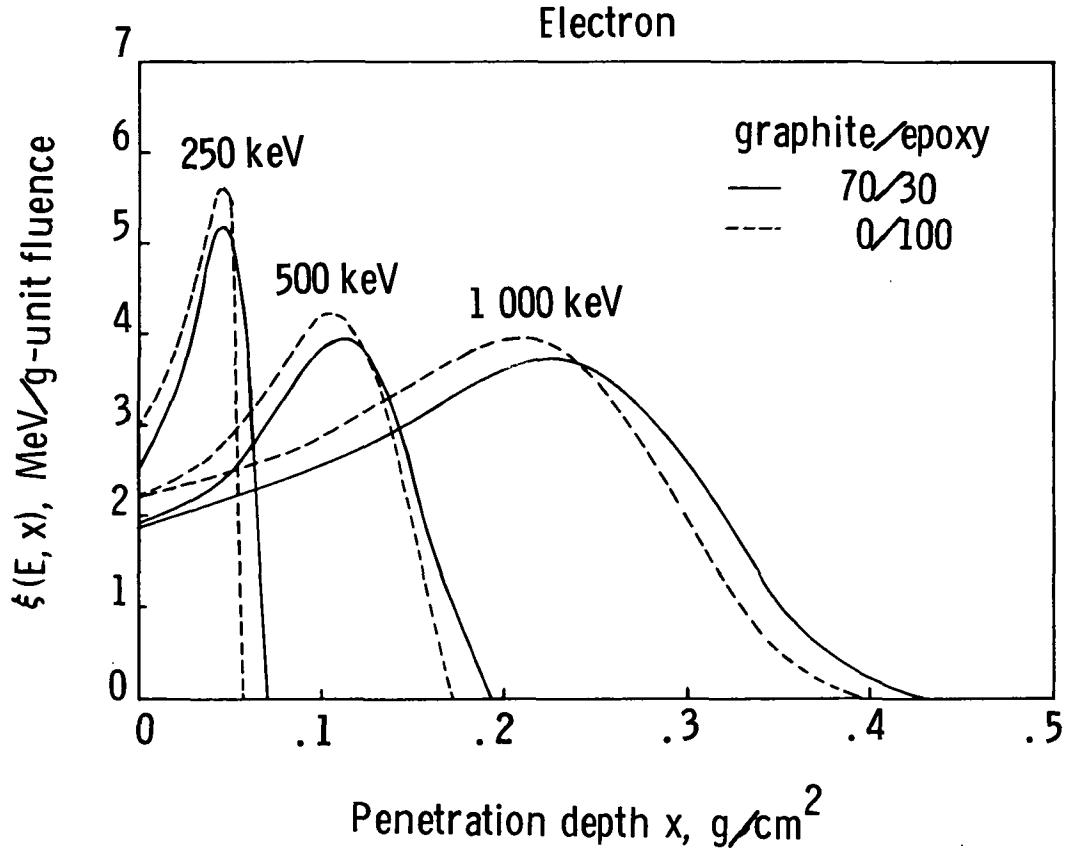

Fig. 3 - Electron energy deposition coefficient for graphite epoxy composite and pure epoxy material.

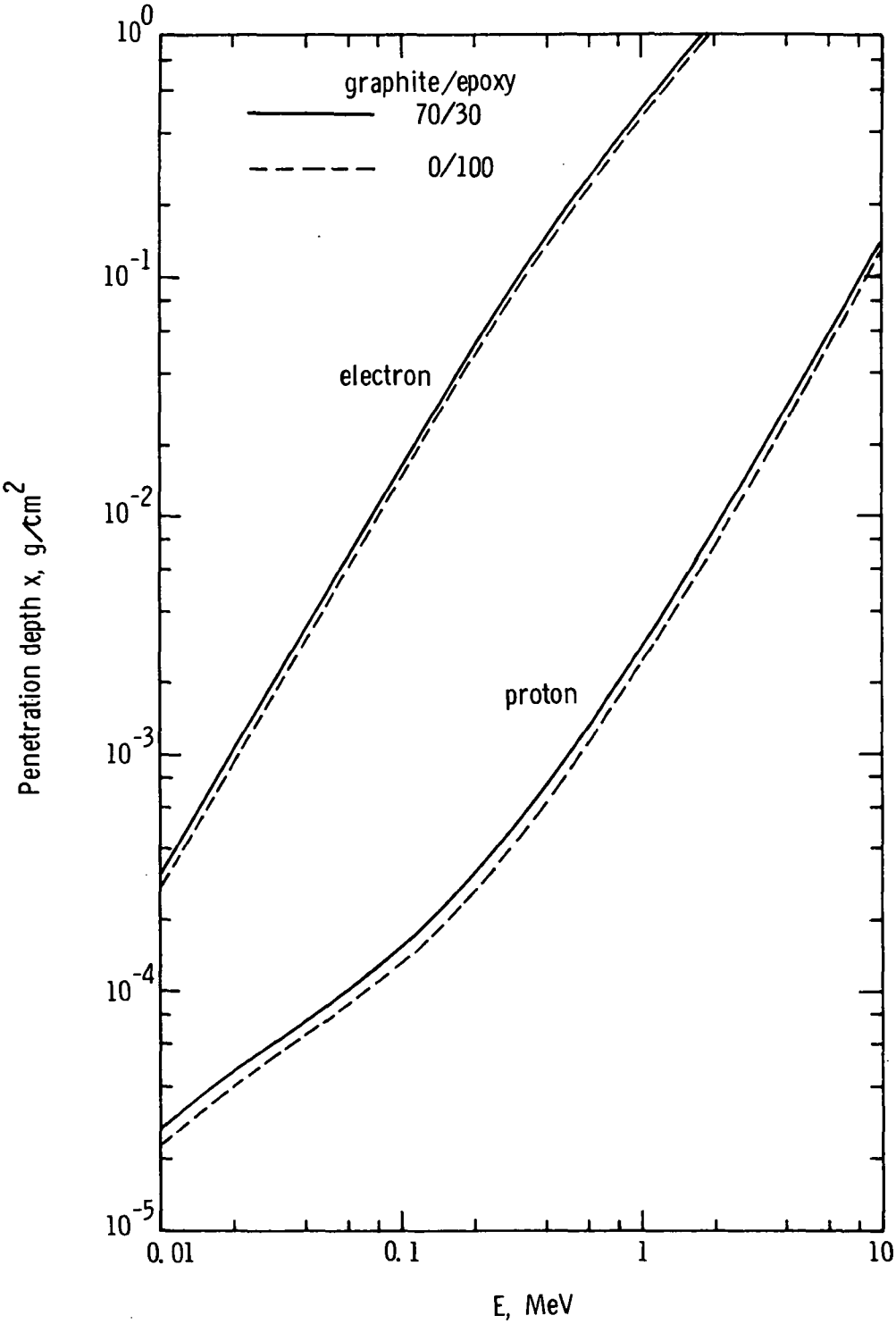

Fig. 4 - Penetration depth as a function of energy for electrons and protons in graphite epoxy composite and pure epoxy materials.

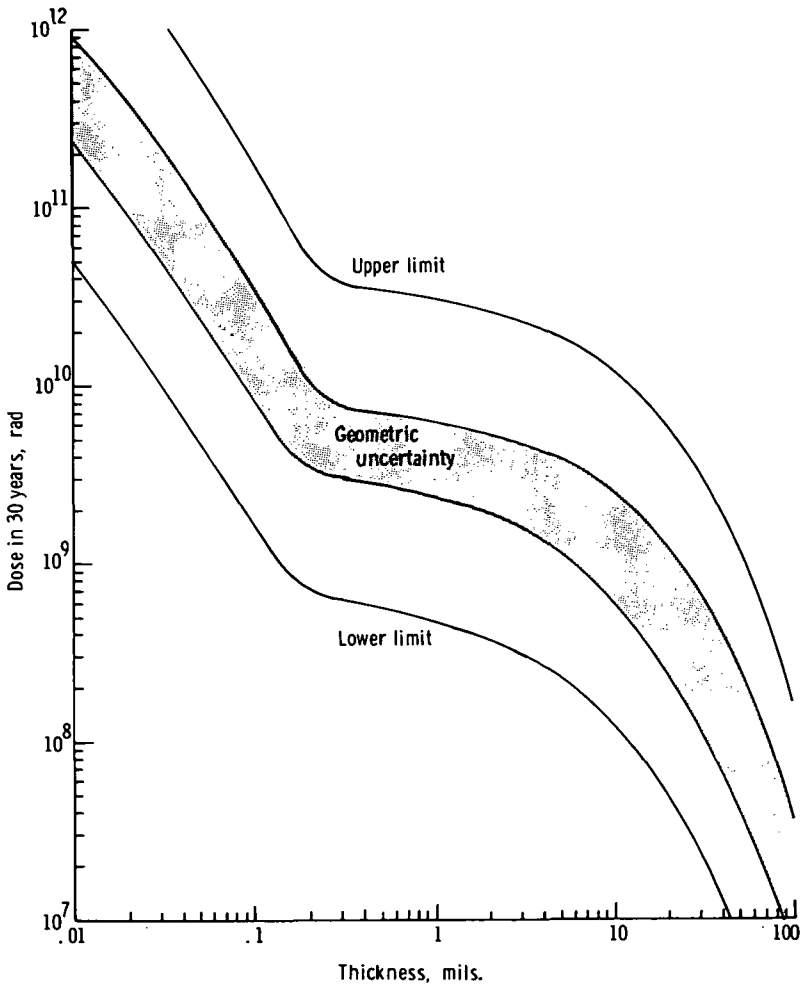

Fig. 5 - Dose in graphite epoxy composite material exposed in geostationary orbit for 30 years.

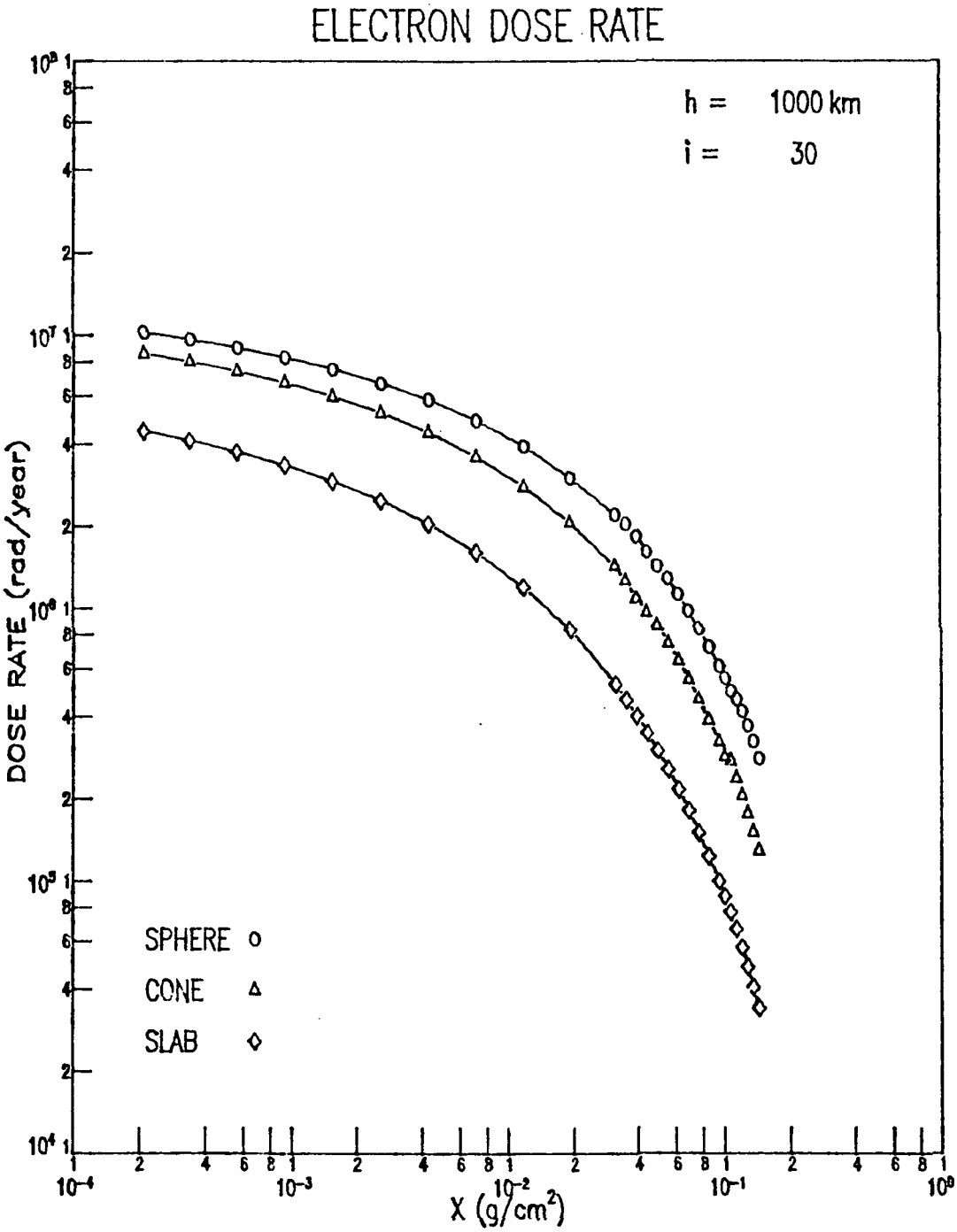

Fig 6-Dose rate in graphite epoxy composite material exposed to electrons in an orbit I 000 Km altitude with 30 degree inclination.

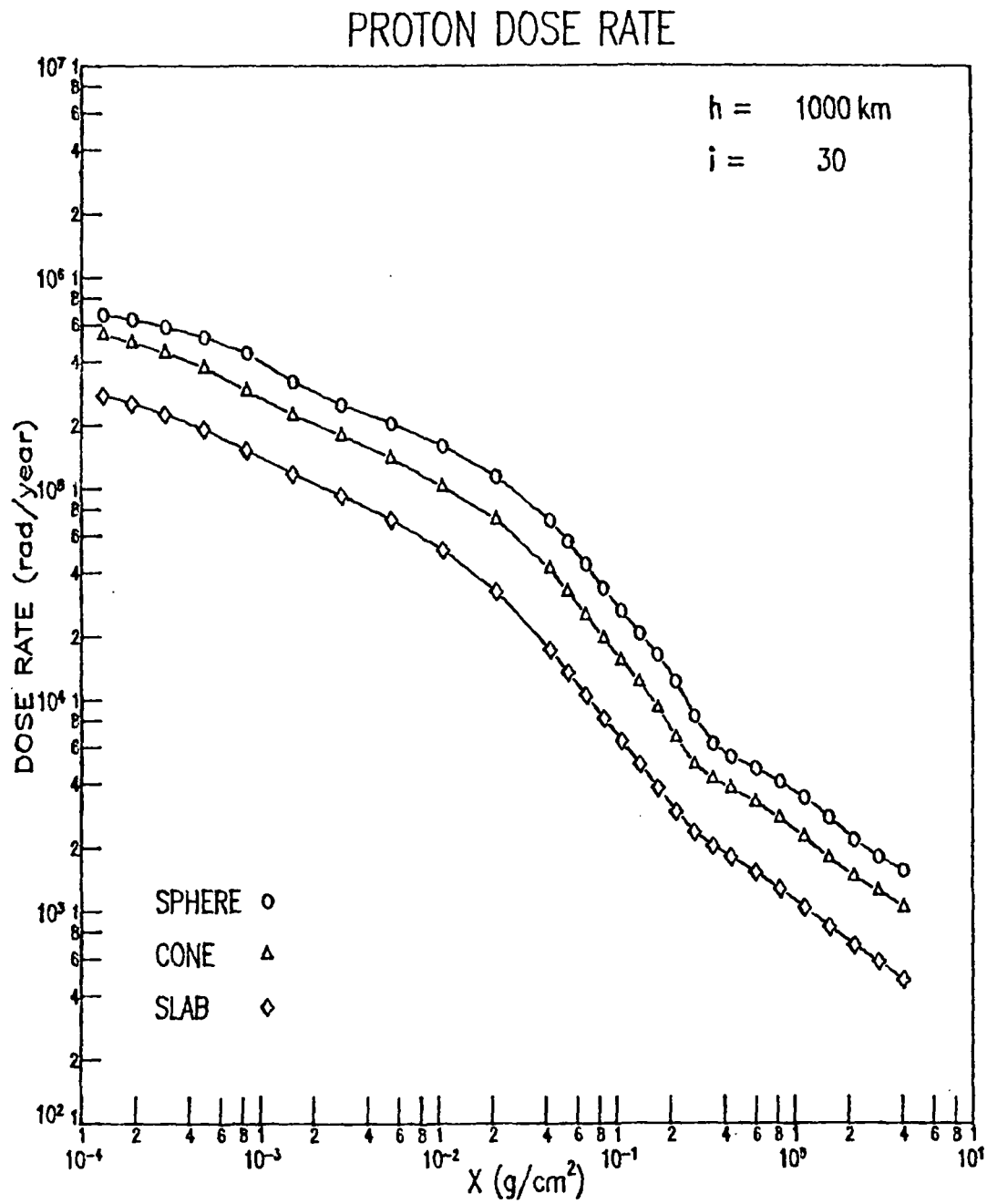

Fig 7- Dose rate in graphite epoxy composite material exposed to protons in an orbit I 000 Km altitude with 30 degree inclination.

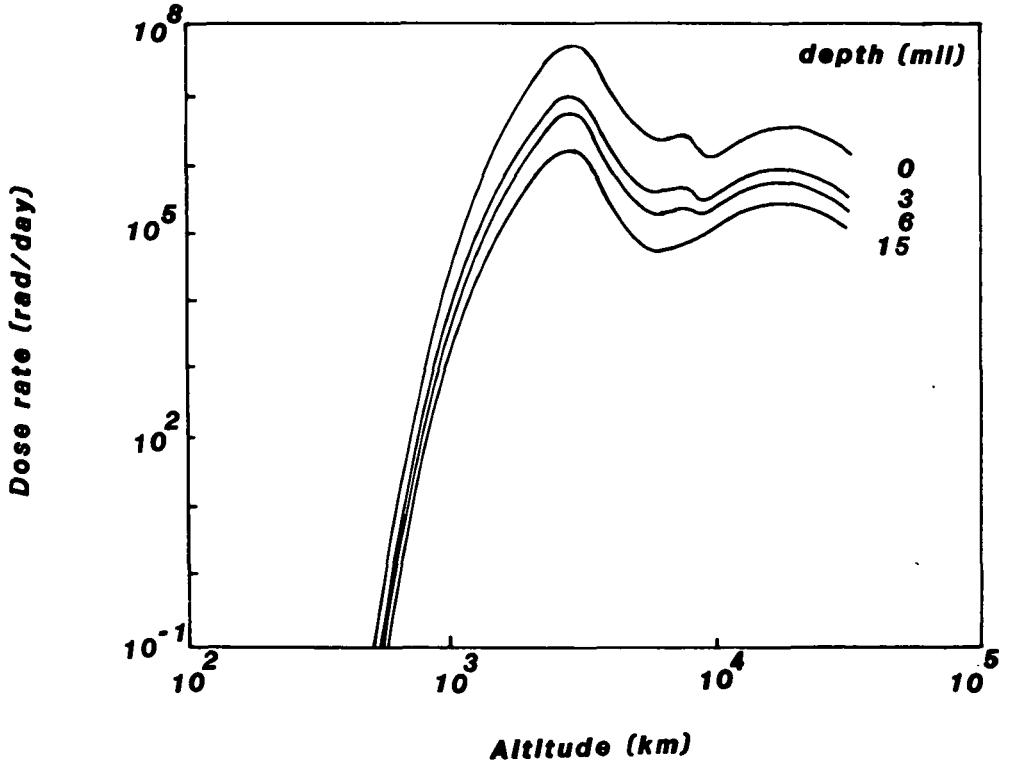

Fig. 8 - Electron dose rate in graphite epoxy composite material exposed in circular orbits at zero inclination.

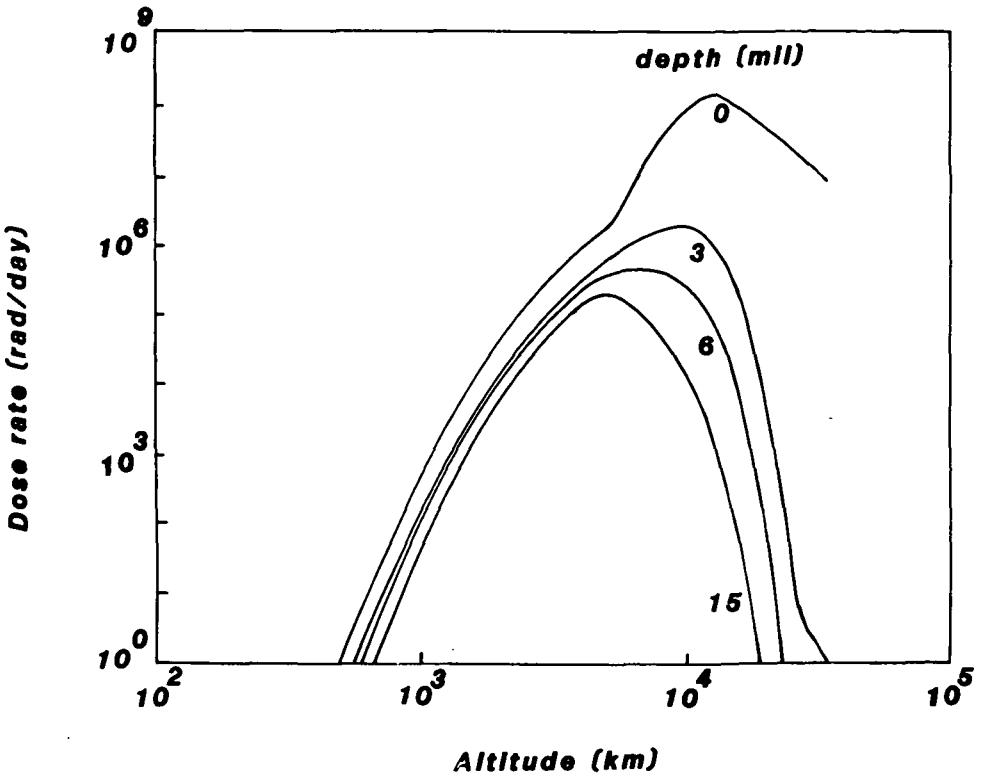

Fig. 9 - Proton dose rate in graphite epoxy composite material exposed in circular orbits at zero inclination.

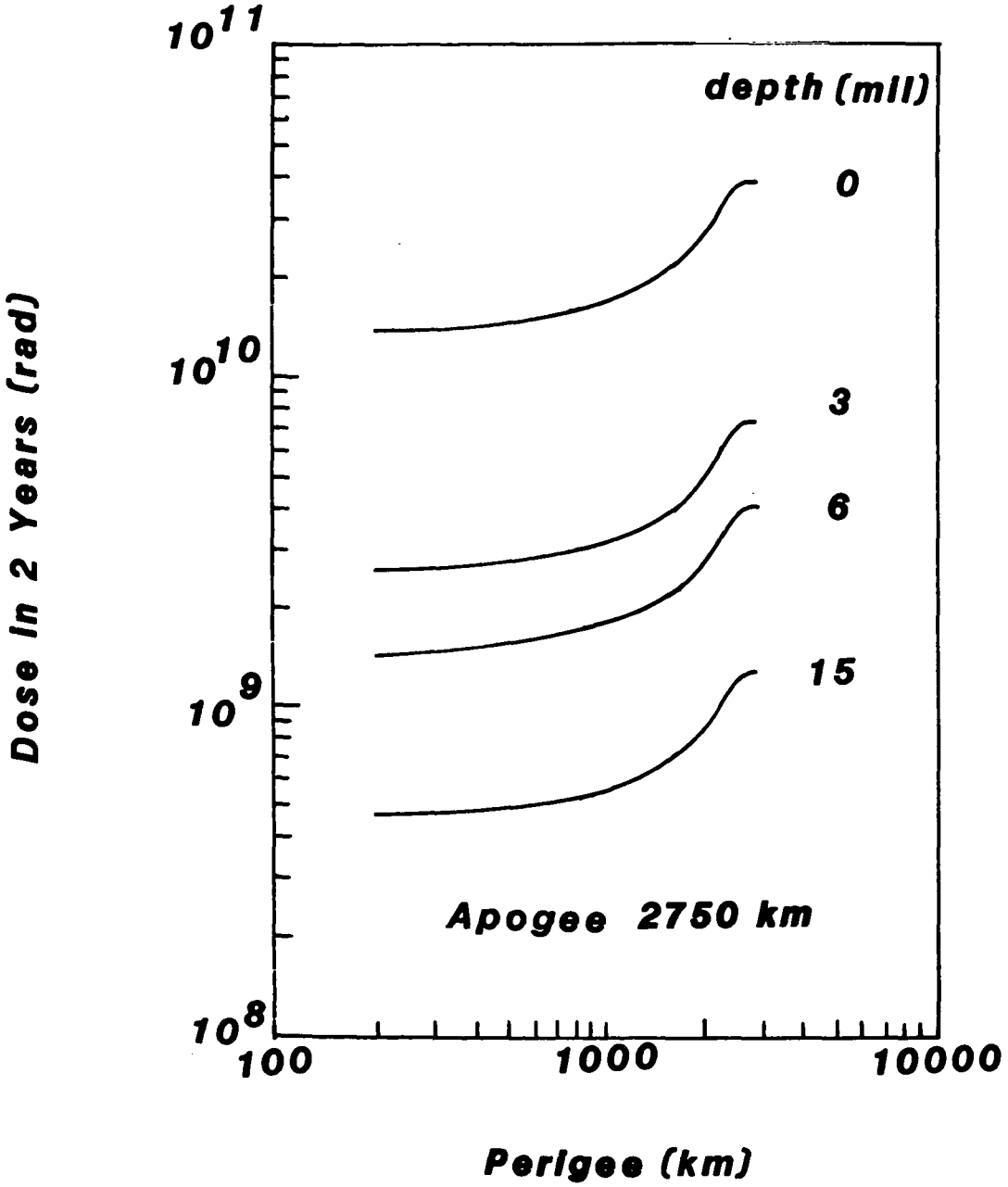

Fig. 10 - Dose in graphite epoxy composite material exposed in elliptical orbits at zero inclination for 2 years.

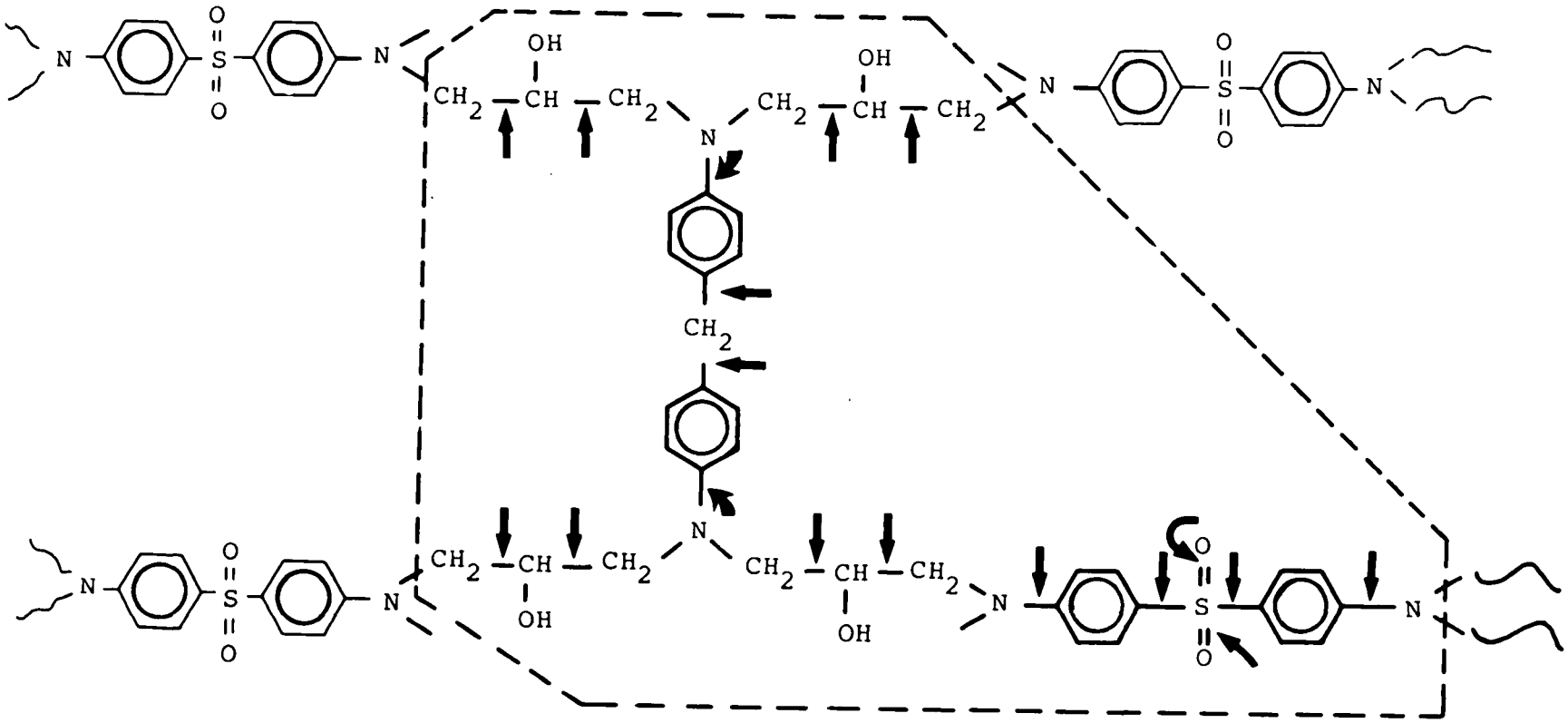

Fig 11. Sites of major dissociative ionization according to electron-impact mass spectra.

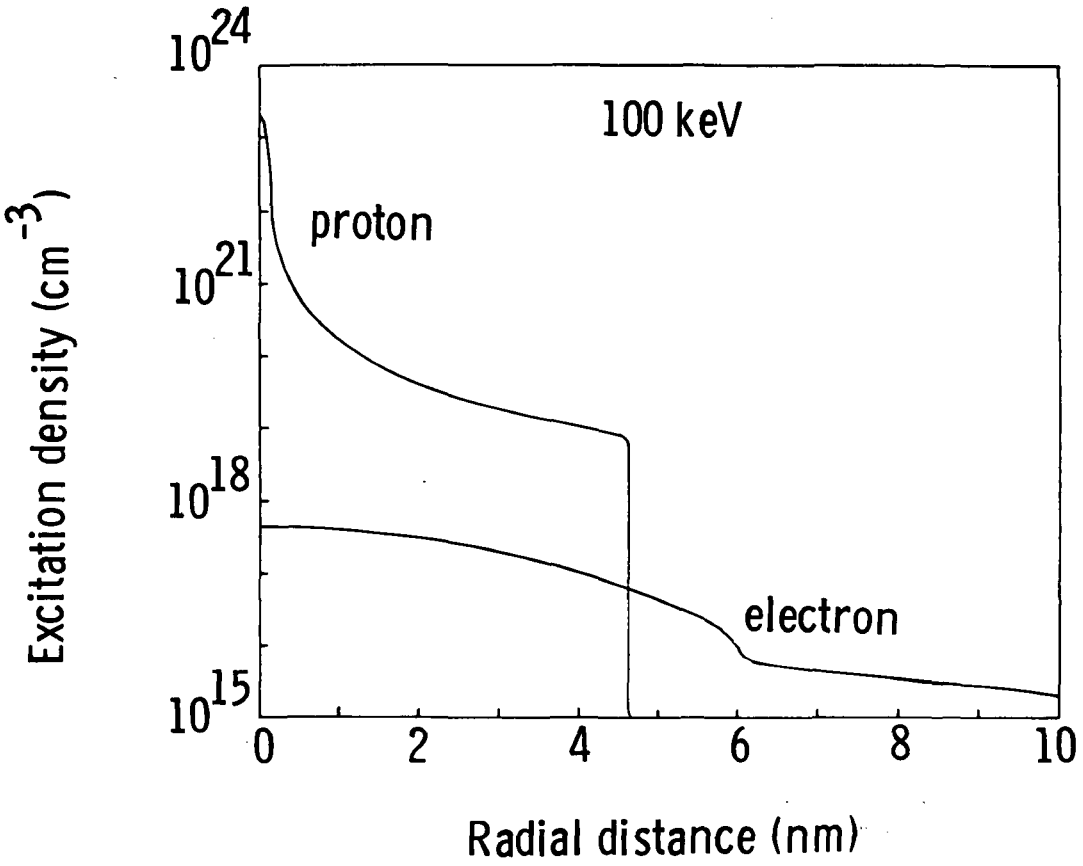

Fig. 12. Excitation density near 100 keV particle path.

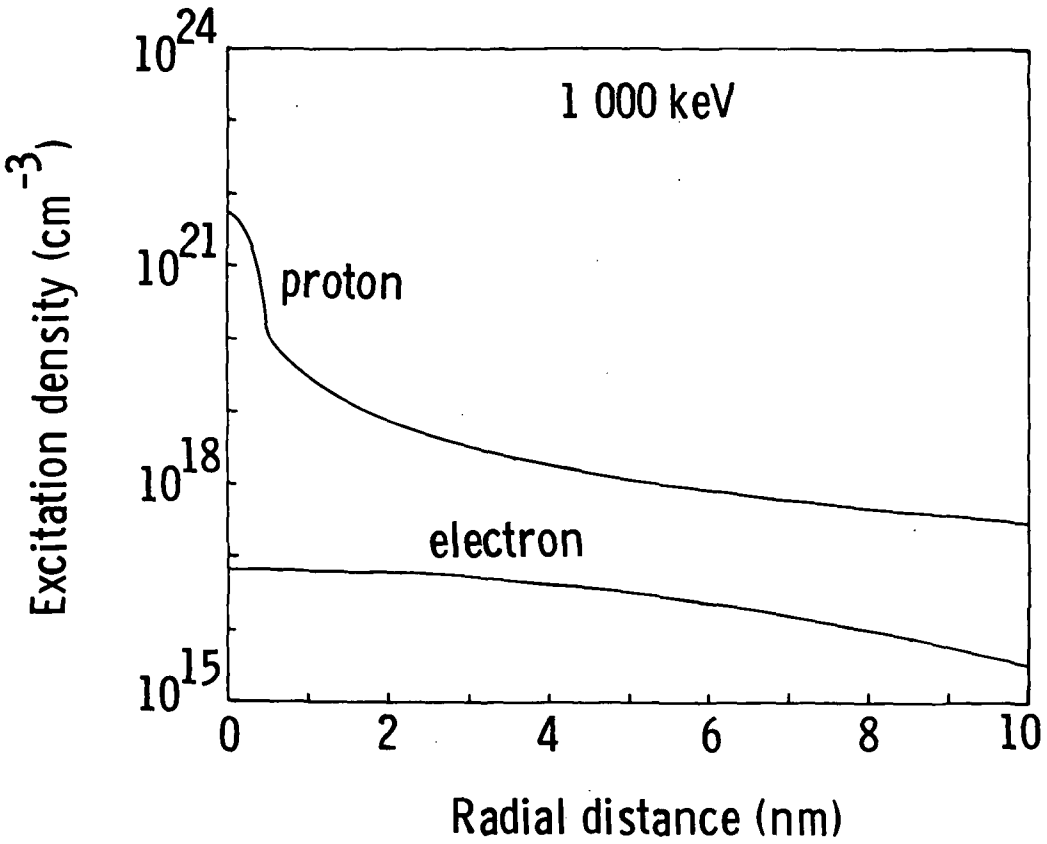

Fig. 13. Excitation density near 1 000 keV particle path.

1. Report No. NASA CR-3618	2. Government Accession No.	3. Recipient's Catalog No.

4. Title and Subtitle	5. Report Date
THEORETICAL STUDIES OF RADIATION EFFECTS IN COMPOSITE MATERIALS FOR SPACE USE	September 1982
	6. Performing Organization Code
7. Author(s)	8. Performing Organization Report No.
C. Ken Chang and Efstathios Kamaratos	
	10. Work Unit No.
9. Performing Organization Name and Address Christopher Newport College Department of Chemistry 50 Shoe Lane Newport News, VA 23606	11. Contract or Grant No. NSG-1614
	13. Type of Report and Period Covered Contractor report
12. Sponsoring Agency Name and Address National Aeronautics and Space Administration Washington, DC 20546	14. Sponsoring Agency Code

15. Supplementary Notes

Langley technical monitor: John W. Wilson

16. Abstract

Tetraglycidyl 4,4'-diamino diphenyl methane epoxy cured with diamino diphenyl sulfone was chosen as a model compound in studying space environmental effects on composite materials. Computer programs were developed to calculate (i) energy deposition coefficients of protons and electrons of various energies at different depths of the material; (ii) ranges of protons and electrons of various energies in the material; and (iii) cumulative doses received by the composite in different geometric shapes placed in orbits of various altitudes and inclination. A preliminary study on accelerated testing was conducted and it was found that an elliptical equitorial orbit of 300 km perigee by 2750 km apogee can accumulate, in 2 years or less, enough radiation dose comparable to geosynchronous environment for 30 years. This orbit is accessible to Shuttle/Orbitor for subsequent retrieval of samples for ground laboratory analysis. The local plasma model was applied to calculate the mean excitation energies for covalent and ionic compounds and were in good agreement with experimental results. Longitudinal and lateral distributions of excited species by electron and proton impact as well as the probability of overlapping of two tracks due to two charged particles within various time intervals were studied. An extensive search on electron-impact mass spectrometry of organic compounds containing similar functional groups as the model compound enabled us in predicting possible bond rupture sites which were in agreement with experiments. Future investigations pertinent to understanding degradation of polymeric materials are planned.

17. Key Words (Suggested by Author(s))	18. Distribution Statement
Graphite epoxy composite,Electrons, Protons,Range,Stopping power,Accelerated testing,Local plasma model,Excited spe species,Bond rupture,Computer programs	Unclassified-Unlimited Subject Category 93

19. Security Classif. (of this report)	20. Security Classif. (of this page)	21. No. of Pages	22. Price
Unclassified	Unclassified	40	A03

For sale by the National Technical Information Service, Springfield, Virginia 22161 NASA-Langley, 1982